

NEW TYPES OF SOLID STATE SOLAR CELLS - ALTERNATIVES FOR SILICON PHOTOVOLTAIC CELLS

AI. ENEŞCA¹ M. COMŞIŢ¹ I. VIŞA¹ A. DUŢĂ¹

Abstract: *The paper is a synthesis of the research reported by the scientific community in the field of new materials used in solid state solar cells. Several chemical compounds seem to attract the attention: CdS, CdTe, CuInS₂, CuInGaSe₂, GaInNAs and TiO₂. All these materials present advantages (chemical stability, wide absorption range, high photosensitivity etc.) and disadvantages (high reflection, intrinsic defects, economically expensive etc.), but the balance of the properties can decide which is the most suitable for the market. For any type of PV cells, the design for in-field applications must consider the specific characteristics of the implementation site, corroborated with the PV materials properties.*

Key words: *solar cell, photovoltaic, solar radiation, conversion.*

1. Introduction

Solar cells based on thin films of polycrystalline materials are promising alternatives when targeting better efficiency/cost ratios than those of solar cells based upon crystalline materials like silicon or gallium arsenide. Therefore, plenty of research has been dedicated to developing heterojunction solar cells, i.e., by putting in contact thin layers of different semiconductor materials grown by low-cost techniques such as chemical bath, spray pyrolysis, electrodepositing and close space vapor transport [5].

It is clear that the large variation in the materials “quality” obtained by the above techniques, or even with the same technique but with different growth conditions, causes

large variations in the behavior of the photovoltaic devices. In this regard, we consider that a better “quality” means improved crystallite sizes, larger mobility and diffusion length of carriers within the grains and increased solar radiation absorption in the active material [2].

Unfortunately, the development of this kind of solar cell is almost empirical since there is some lack of knowledge on the material properties with which these devices are manufactured. Hence, it is common that researchers in some laboratories attempt to reproduce the structure reported in another one, without considering the appropriate design, and the particular properties of the solar cell materials developed in their own laboratory [16].

¹ Centre “Product Design for Sustainable Development”, *Transilvania* University of Braşov.

This paper presents a synthesis of different solid state solar cells reported in the literature. The differences consist, not only, on the production technique but also on the chemical composition and geometrical structure of the cells. High-efficiency CIGS and CdTe devices are generally manufactured with such bi-layer structures, consisting of a highly conducting layer for low-resistance due to contact and lateral current collection and a much thinner high-resistivity layer (called buffer layer) of a suitable material, to minimize forward current through pinholes in the window layer. By incorporating a 50 nm thick resistive SnO_2 , In_2O_3 , ZnO , or Zn_2SnO_4 layer, the CdS layer thickness can be reduced to 80 nm, which significantly improves the blue response of the CdTe devices. The presence of the smoother high-resistive layer also improves the CdS film morphology by providing large grains during chemical bath deposition (CBD) [4], [7], [9].

2. Solid State Solar Cells

2.1. CdS-CdTe Solar Cells

The CdTe-CdSe solar cells were among the first prepared without using silicon and are part of the II-VI class of photovoltaic converters. The team lead by X. Wu at NREL in the USA has achieved the highest efficiency for this type of solar cells. In Figure 1 shows the structure and approximate thickness of each layer in the device that was reported with a 16.5% efficiency [11].

Notice the presence of the mentioned CdTO (TO - tin oxide) and ZnTO bilayer for the TCO. Notice also that they have used a 10 μm CdTe layer, but with a very thin CdS layer below 0.1 μm . The graphite contact at the back of the CdTe layer usually contains Cu as this seems to be needed for good ohmic contacts on the p-type CdTe.

For their highest efficiency solar cell: V_{oc} (open circuit voltage) = 845 mV, J_{sc} (short circuit current density) = 25.88 mA/cm^2 , FF (fill factor) = 75.5%, η (efficiency) = 16.5% [11].

CdS/CdTe solar cells, both CdS and CdTe are polycrystalline and the physical parameters vary depending on the growth conditions as well as the growth techniques. The minimum thickness for the CdTe film to absorb 90% of the incident spectrum is approximately 1 μm . To simplify the analysis, a simple structure of CdS/CdS_{1-x}Te_x/CdTe has been used. The structure is shown in Figure 2 [1].

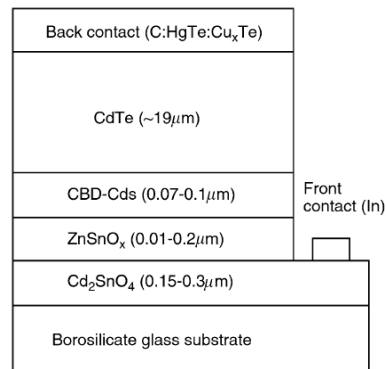


Fig. 1. *CTO/ZTO/CdS/CdTe* record efficiency solar cell device structure [11]

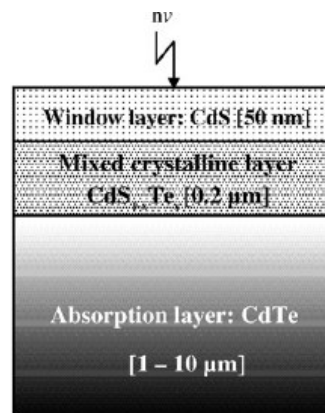


Fig. 2. *The structure of CdS/CdTe* solar cell [1]

The first result obtained from the calculation is the effect of CdTe thickness on the solar cell characteristics. The CdTe thickness was changed from 0.25 to 10 μm . As shown in Figure 3, all the solar cell characteristics are almost unchanged at thicknesses of 3-10 μm . However, the open-circuit voltage (V_{OC}) and the short-circuit current (J_{SC}) decrease drastically below the thickness of 2 μm . It can be seen that the long-wavelength spectral response decreases with the decrease of CdTe thickness [1].

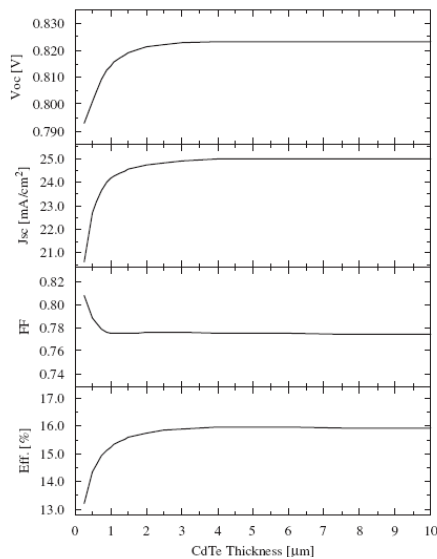


Fig. 3. *The effect of the CdTe thickness reduction on the solar cell characteristics [1]*

2.2. GaInNAs Solar Cell

Another class of thin film solar cells, the III-V cells, using semiconductors resulted from the combination of group III materials (Ga, In, Sb) with materials from group V (N, P, As). The growing interest to find new materials for solid state solar cells made it possible to introduce arsenate (As) as a key component in photovoltaic conversion. Y. Kamikawa-Shimizu & co. have obtained

thin GaInNAs films and p-i-n homojunction solar cell structures on GaAs (001) substrates by H-MBE using a rf-plasma as the active nitrogen source. Atomic H is generated using a hand-assembled cracking cell with a tungsten filament heated by direct current in passing hydrogen gas. The cracking ratio of molecular H_2 to atomic H is controlled by the power supplied to the tungsten filament. The H_2 gas flow is accurately controlled using a variable leak valve. Figure 4 shows the schematic structure of a p-i-n homojunction GaInNAs solar cell. Each substrate was first subjected to surface cleaning at 580 $^{\circ}\text{C}$ for 30 min with atomic H irradiation. After the surface cleaning, a 0.5- μm -thick n^+ -GaAs buffer layer ($n = 2 \times 10^{18} \text{ cm}^{-3}$) was grown at 580 $^{\circ}\text{C}$.

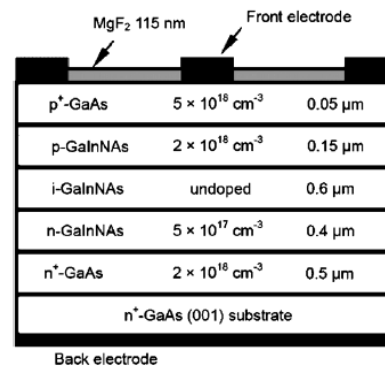


Fig. 4. *Schematic layer structure of p-i-n homojunction GaInNAs solar cell fabricated in this work [8]*

Then, a Si-doped 0.4- μm -thick n-GaInNAs base layer ($n = 5 \times 10^{17} \text{ cm}^{-3}$), followed by a 0.6- μm -thick undoped GaInNAs layer, a Be-doped 0.15- μm -thick p-GaInNAs emitter layer ($p = 2 \times 10^{18} \text{ cm}^{-3}$), and finally a 0.05- μm -thick p⁺-GaAs contact layer ($p = 5 \times 10^{18} \text{ cm}^{-3}$) were consecutively grown at 500 or 520 $^{\circ}\text{C}$. The conditions of atomic H irradiation for the p-i-n GaInNAs region and GaAs contact layer were varied by changing both the flow rate of H_2 gas

and the cracking efficiency into H atoms. All samples were grown with irradiation of atomic H under the same conditions up to the GaAs buffer layer. During the growth of GaInNAs region, the rf power and N_2 flow rate were set to 80 W and 1 sccm, and the growth rate was 0.9 $\mu\text{m}/\text{h}$ for GaInNAs and 1.0 $\mu\text{m}/\text{h}$ for GaAs layers. The arsenic back pressure was kept at $\sim 2 \times 10^{-6}$ Torr through out the growth. For solar cell fabrication, AuZ n alloy and In were used as the top and the bottom contacts, respectively. A standard anti-reflection coating with MgF_2 was employed in 0.25 cm^2 sized solar cells [8].

K. Nishioka & co. proposed a new configuration consisting of a InGaP/InGaAs/Ge triple-junction solar cell. The subcells (InGaP, InGaAs and Ge junctions) of the triple-junction solar cell were grown on a p-type Ge substrate by metal-organic chemical vapor deposition (see Figure 5). The $\text{In}_{0.49}\text{Ga}_{0.51}\text{P}$ top, $\text{In}_{0.01}\text{Ga}_{0.99}\text{As}$ middle, and Ge bottom subcells were all lattice matched. The InGaP subcell was connected to the InGaAs subcell by a p-AlGaAs/n-InGaP tunnel junction. The InGaAs subcell was connected to the Ge subcell by a p-GaAs/n-GaAs tunnel junction [12].

In Figure 6 shows the measured spectral response (external quantum efficiency (EQE)) of the InGaP/InGaAs/Ge triple-junction solar cell. The InGaP/InGaAs/Ge triple-junction solar cell can absorb light of a wide wavelength and converts it into electricity [12].

Basically, increasing the number of junctions targets the extension of the radiation spectra useful for the PV cell, consequently, an increased photovoltaic conversion and a higher electrical response. As described, manufacturing these types of cells requires accurate technologies and rather extreme parameters. This obviously raises the costs and only a significant increase in efficiency can justify the investment.

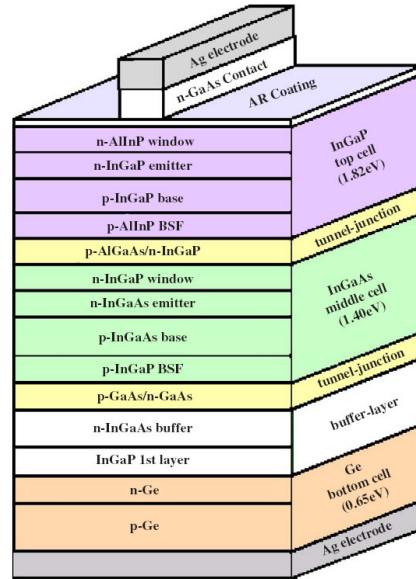


Fig. 5. Schematic of an InGaP/InGaAs/Ge triple-junction solar cell [12]

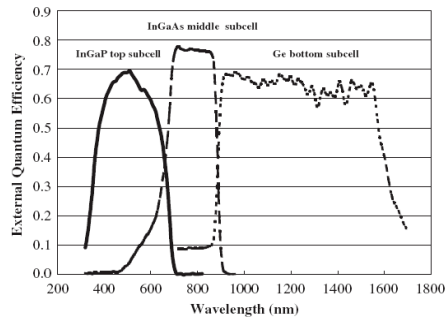


Fig. 6. External quantum efficiency of an InGaP/InGaAs/Ge triple-junction solar cell [12]

2.3. CIGS Solar Cell

S. Ishizuka & co. have investigated the thin film growth of CIGS and post CIGS deposition processes with the goal of achieving higher efficiencies from wider-gap CIGS thin film solar cells. The research was focused on a Ga composition x of around 0.5, which corresponds to $E_g = 1.3$ eV. Although the effects and roles of buffer

layers such as CdS and Zn-related materials between the CIGS and the transparent conductive oxide (TCO) layers have been extensively studied and discussed in the literature, so far there have been no detailed studies and discussions concerning the use of highly resistive *i*-ZnO layers, which are commonly introduced for the prevention of leakage current, between the buffer layers of CIGS thin films and the TCO as shown in Figure 7, [6].

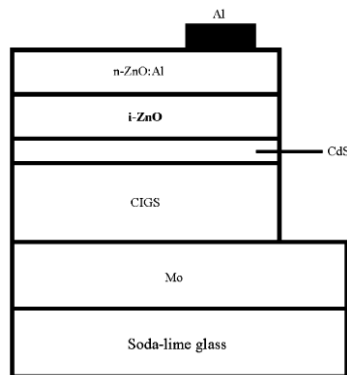


Fig. 7. *Schematic illustration of the CIGS solar cell structure* [6]

In Figure 8 the J-V curve shapes changed with *i*-ZnO layers were thinner than the critical thickness of 70 nm, the leakage current was found to increase and the FF (fill factor) worsened as shown in Figure 8a. On the other hand, when the *i*-ZnO layers were thicker than the critical thickness, current density in the solar cell circuit gradually decreased with increasing the *i*-ZnO thickness due to an increase in serial resistance, consequently, the FF worsened as shown in Figure 8b. It was found from these results that the FF worsened and cell efficiencies degraded in each case where *i*-ZnO layers were thinner or thicker than the critical thickness, proving this parameter as one of the most important in the CIGS design [6].

Similar investigations were done by C.Y. Shi & co., on the influence of ZnO film

thickness on the CIGS solar cell. In their study, ZnO layers were deposited on 50- μm -thick SS (stainless steel) substrates as diffusion barriers for flexible CIGS solar cells. Then the flexible CIGS solar cell on SS substrate was fabricated with a structure of SS/ZnO/Mo/CIGS/CdS/*i*-ZnO/ZnO:Al (as shown in Figure 9). ZnO layers were deposited as diffusion barriers by DC magnetron sputtering from a pure Zn target under an Ar/O₂ atmosphere on SS substrates. The film thickness ranged from 1 to 3 μm . The 0.89 μm Mo back electrodes were sequentially deposited on the ZnO-coated SS substrates by DC sputtering. The CIGS absorber layers with a thickness of about 2.3 μm were prepared by a three-stage process at a temperature of about 570 °C.

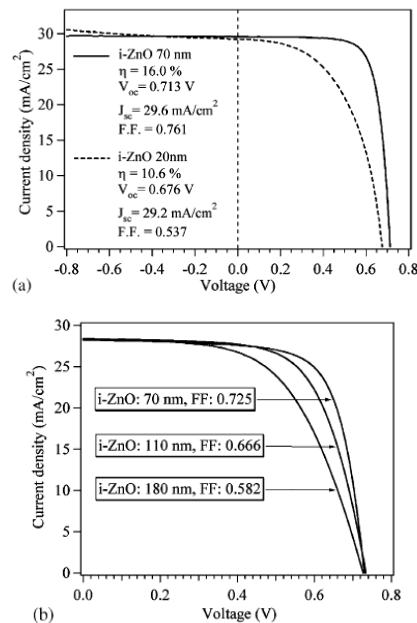


Fig. 8. *J-V characteristics of CIGS cells fabricated with *i*-ZnO layer thinner than 70 nm (a) and thicker than 70 nm (b)* [6]

Device fabrication was continued by the growth of the CdS buffer layer via chemical bath deposition (CBD) and the ZnO window bilayer was grown by

intermediate frequency magnetron sputtering. The 500 Å thick i-ZnO was deposited from an intrinsic ZnO target under an Ar/O₂ atmosphere, and the 3000 Å thick ZnO:Al layer was deposited from an Al₂O₃-doped ZnO target (2.5 wt%) under an argon atmosphere. Moreover, Ni/Al grids were evaporated on to the finished devices in order to facilitate current collection. As reference, CIGS thin film solar cells were additionally fabricated on SS substrates without ZnO diffusion [13].

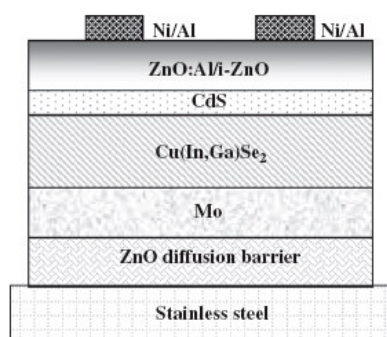


Fig. 9. Schematic structure of CIGS solar cell on SS substrate with ZnO diffusion barrier [13]

2.4. TiO₂ Solar Cell

The dye sensitized solar cells, developed by M. Graetzel and co-workers attracted a lot of attention from the very beginning, because it exhibited a quite large efficiency (close to 12%), with low-cost material. Research was dedicated to optimize the dye, the interface, the oxidation/reduction couple and finally the cell design, with the aim of reducing the drawbacks, mainly related to the rather short time of functioning (up to 10 years). Recently, Z. Tachan & co. reported a new and simple DSSC (dye-sensitized solar cell) design based on tubes. Glass tubes were coated from the inner side with a conducting transparent FTO layer onto which the mesoporous TiO₂ film was deposited. Across-section of these DSSTs is

schematically shown in Figure 10a. As counter electrodes, FTO-coated glass rods were used, onto which a Pt layer was sputtered. The round shape of the DSSTs opened a way to transfer the opaque current collector to the back side of the cell, thus avoiding the losses associated with shading from collector lines (Figure 10b). DSSTs drastically reduce the area for sealing and can be used as building blocks for dye-sensitized solar panels in which individual cells (tubes) are easily mounted and replaced. The group reported the production of a DSST and characterized a surface segment with an area of 0.7 cm² under direct illumination of simulated sunlight to compare its performance to flat DSSCs [15].

The interest for SSSC based on TiO₂ layer lead to various synthesis routs, such as that reported by E. Stahatos & co who used the Degussa P25 powder as seeding agent for further TiO₂ preparation. The synthesis of TiO₂ layer was made using one gram of P25-TiO₂ powder added in 10 mL of ethanol followed by magnetic stirring to obtain a homogeneous dispersion. No surfactants were used as templates to the solution. TTIP was mixed in the previous dispersion in various concentrations (varied from 0.017 to 0.18 M). After several minutes, the dispersion was ready to be used either on glass or plastic substrates [14].

Films with effective surface area of around 1 cm² were formed on glass substrate by dip coating (12370.5 cm/min withdrawal velocity).

The TiO₂ films prepared by the above procedure on FTO glass or ITO-PET plastic substrates were immersed into an 1 mM ethanolic solution of RuL₂(NCS)₂ (dye solution) and were left there overnight [14].

The current-voltage (J-V) characteristic curves of quasi-solid-state DSSCs for the room temperature TiO₂ films with optimum TTIP content prepared on glass and plastic conductive substrates are presented in Figure 11, [14].

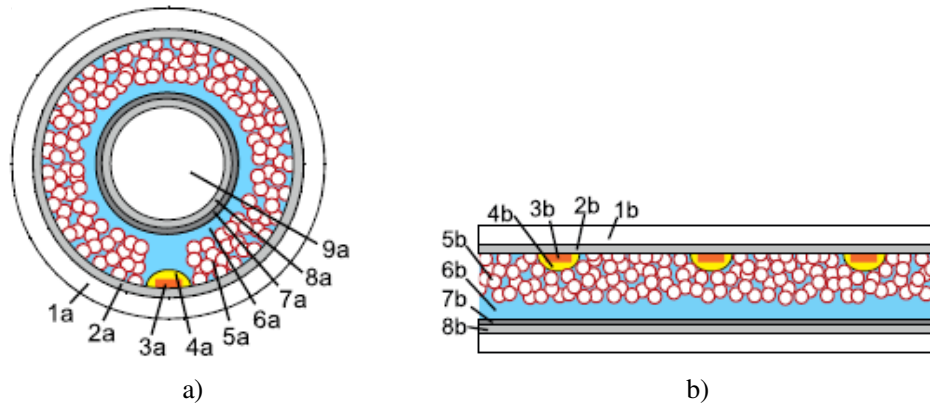


Fig. 10. a) Schematic cross-section of a dye-sensitized solar tube (DSST) showing the glass tube (1a), the FTO layer deposited by spray pyrolysis (2a), a highly conducting current collector attached to the FTO on the bottom side inside the DSST (3a) and a polymer layer, which is protecting the current collector (4a).

The mesoporous dye-sensitized TiO_2 film (5a) deposited onto the FTO is immersed into the redox electrolyte (6a). The circuit is closed by a counter electrode consisting of a sputtered Pt layer (7a) on top of a sprayed FTO film (8a), deposited onto a quartz rod (9a);

b) Schematic drawing of a conventional DSSC consisting of a flat glass substrate (1b), covered with commercial FTO (2b). The opaque current collector (3b) with a protective coating (4b) is partially blocking the incident light. The dye-sensitized TiO_2 film (5b) is immersed into electrolyte (6b) which is in contact with Pt (7b) deposited on flat FTO glass (8b) [15]

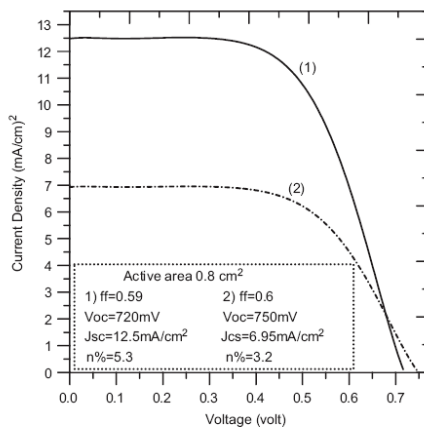


Fig. 11. J-V curves at I_{sun} for the DSSCs containing the as-prepared low-temperature nanocrystalline TiO_2 film on (1) FTO glass and (2) ITO-PET plastic substrate [14]

Quasi-solid-state DSSCs employing 2 μm thick TiO_2 electrodes prepared at low temperature with optimum TTIP quantity were compared with those that were made with TiO_2 films developed at high temperature.

The efficiency of the cells with the as-prepared films at room temperature was 23% lower than that of the cells with TiO_2 sintered at high temperature. This result was expected as TiO_2 particles treated at high temperature give improved charge collection efficiencies because of networking with strong bridges. However, the disadvantage of somewhat lower efficiency is overcome by the lower anticipated cost of preparation for the TiO_2 electrode. Manufacturing processes which truly represent significant cost savings will

only be realized when high speed, roll-to-roll coating operations are devised. This requires low cost, flexible polymer film, and therefore rapid, low-temperature deposition techniques for TiO₂ films. Furthermore, gel electrolytes are a promising approach to combine the high-ionic conductivity of liquids while reducing the risk of leaks and minimizing sealing problems in DSSCs [14].

2.5. ETA and 3D Solid State Solar Cells

Following the first ETA cell reported by O'Brien, work was dedicated to develop new, thin film-based, solid state solar cells, where both the n-type and the p-type semiconductors are solid. The group in the

Transilvania University of Braşov, Romania, developed research on these types of cells, aiming to produce these cells by a single deposition technique, low-cost, reproducible and accurate. Spray pyrolysis deposition was employed for obtaining various structures [10]:

1. TCO/dense TiO₂/In₂S₃(15 sp)/CuSbS₂/graphite;
2. TCO/dense TiO₂/nanoporous TiO₂(20 sp)/In₂S₃(15 sp)/CuSbS₂/graphite;
3. TCO/dense TiO₂/nanoporous TiO₂(30 sp)/In₂S₃(15 sp)/CuSbS₂/graphite;
4. TCO/dense TiO₂/nanoporous TiO₂(40 sp)/In₂S₃(15 sp)/CuSbS₂/graphite.

The output parameters for these cells are presented in Table 1.

Output parameter for solid state solar cells

Table 1

Sample Cell	V_{oc} [mV]	I_{sc} [A]	V_{max} [mV]	I_{max} [A]	FF
1	253	$7.54 \cdot 10^{-5}$	132	$4.50 \cdot 10^{-5}$	0.311
2	210	$8.13 \cdot 10^{-5}$	117	$4.64 \cdot 10^{-5}$	0.318
3	193	$8.05 \cdot 10^{-5}$	104	$4.74 \cdot 10^{-5}$	0.317
4	155	$5.50 \cdot 10^{-5}$	84	$3.12 \cdot 10^{-5}$	0.307

These type of solar cells can significantly improve their efficiency when heated; therefore, they represent a good alternative for concentrating radiation, when - along with a multiplied amount of input radiation also results heat. In silicon cells this heat is responsible for a drop in efficiency.

2.6. Solar Cells Operation

The PV manufacturers are concentrating on optimizing the PV cells/modules design. The output parameter are registered under standard conditions but, the cells and the modules are seldom functioning under a constant irradiation of 1000 W/m². Variable solar radiation intensity, clouding, shadowing, dusting, heating (conductive, convective or radiative) are only few of the parameters that are strongly linked to the

implementation conditions.

It is therefore important, before starting the design of a new PV array/plant to carefully evaluate the specific characteristics of the implementation location. A recent study [3], showed that although June, July and August are the months with the highest solar energy input, in Brasov, the highest efficiencies were attained, for a 10 kWp array, during April when a combination of radiation amount and low temperature lead to the (actually) optimized conditions.

When thinking on concentrating PV systems, this type of data is even more important. While fully solid state solar cells will increase their charge carrier mobility with temperature, the silicon cells act oppositely and the DSSC may lose the solvent of the oxidation-reduction couple, thus shortening their life.

3. Conclusions

The research interest in the field of solid state solar cells have imposed new challenges in finding and optimizing new materials with advanced opto-electronic properties. The CdS-CdTe solar cells have exhibited more than 16% efficiency but the CdS life time has to be improved. The TiO₂ solar cells have a good chemical stability but a lower efficiency (around 10%). The CIGS and GaInNAs solar cells are considered the most promising materials for replacing silicon in photovoltaic applications but the price is still too high for future implementation in developing countries.

The possibility to use low-cost techniques for TiO₂ deposition and to improve the photovoltaic conversion can be the key for the next generation of photovoltaic systems. Specific PV system design must also consider the implementation conditions, including weather data along with pollution data (particulate, PM10).

Acknowledgements

This paper is supported by the Sectoral Operational Programme Human Resources Development (SOP HRD) Post-Doctoral Studies, financed from the European Social Fund and by the Romanian Government under the contract number POSDRU 59323.

References

1. Amin, N., Sopian, K., Konagai, M.: *Numerical Modeling of CdS/CdTe and CdS/CdTe/ZnTe Solar Cells as a Function of CdTe Thickness*. In: *Solar Energy Materials & Solar Cells* **91** (2007), p. 1202-1208.
2. Dhere, N.G.: *Present Status and Future Prospects of CIGSS Thin Film Solar Cells*. In: *Solar Energy Materials & Solar Cells* **90** (2006), p. 2181-2190.
3. Eneșca, Al., Comșîț, M., Vișa, I., Duță, A.: *Photovoltaic Efficiency of a Grid Connected 10 kWp System Implemented in the Brasov Area*. In: *Proceedings of OPTIM, IEEE Proceedings, 2010*, p. 342.
4. Fuke, N., Fukui, A., Islam, A., Komiya, R., Yamanaka, R., Harima, H., Han, L.: *Influence of TiO₂/Electrode Interface on Electron Transport Properties in Back Contact Dye-Sensitized Solar Cells*. In: *Solar Energy Materials & Solar Cells* **93** (2009), p. 720-724.
5. Hegedus, S.S., McCandles, B.E.: *CdTe Contacts for CdTe/CdS Solar Cells: Effect of Cu Thickness, Surface Preparation and Recontacting on Device Performance and Stability*. In: *Solar Energy Materials & Solar Cells* **88** (2005), p. 75-95.
6. Ishizuka, S., Sakurai, K., Yamada, A., et al.: *Fabrication of Wide-Gap Cu(In_{1-x}Ga_x)Se₂ Thin Film Solar Cells: A Study on the Correlation of Cell Performance with Highly Resistive i-ZnO Layer Thickness*. In: *Solar Energy Materials & Solar Cells* **87** (2005), p. 541-548.
7. Jianmin, H., Yiyong, W., Jingdong, X., Dezhuang, Y., Zhongwei, Z.: *Degradation Behaviors of Electrical Properties of GaInP/GaAs/Ge Solar Cells under <200 keV Proton Irradiation*. In: *Solar Energy Materials & Solar Cells* **92** (2008), p. 1652-1656.
8. Kamikawa-Shimizu, Y., Niki, S., Okada, Y.: *Fabrication of Homojunction GaInNAs Solar Cells by Atomic Hydrogen-Assisted Molecular Beam Epitaxy*. In: *Solar Energy Materials & Solar Cells* **93** (2009), p. 1120-1123.
9. Ken, L., Dolmanan, S.B. Shen, L., et al.: *Degradation Mechanism of ZnO-Based Dye-Sensitized Solar Cells*. In:

- Solar Energy Materials & Solar Cells **94** (2010), p. 323-326.
10. Manolache, S., Duta, A.: *Three-Dimensional (3d) Solar Cell FTO/TiO₂/CuSbS₂/graphite*. In: European PV Conference Proceedings, 2007, p. 243.
 11. Morales-Acevedo, A.: *Can We Improve the Record Efficiency of CdS/CdTe Solar Cells?* In: Solar Energy Materials & Solar Cells **90** (2006), p. 2213-2220.
 12. Nishioka, K., Takamoto, T., Agui, T., et al.: *Evaluation of InGaP/InGaAs/Ge Triple-Junction Solar Cell and Optimization of Solar Cell's Structure Focusing on Series Resistance for High-Efficiency Concentrator Photovoltaic Systems*. In: Solar Energy Materials & Solar Cells **90** (2006), p. 1308-1321.
 13. Shi, C.Y., Sun, Y., He, Q., et al.: *Cu(In,Ga)Se₂ Solar Cells On Stainless-Steel Substrates Covered with ZnO Diffusion Barriers*. In: Solar Energy Materials & Solar Cells **93** (2009), p. 654-656.
 14. Stathatos, E., Chen, Y., Dionysiou, D.D.: *Quasi-Solid-State Dye-Sensitized Solar Cells Employing Nanocrystalline TiO₂ Films Made At Low Temperature*. In: Solar Energy Materials & Solar Cells **92** (2008), p. 1358-1365.
 15. Tachan, Z., Ruhle, S., Zaban, A.: *Dye-Sensitized Solar Tubes: A New Solar Cell Design for Efficient Current Collection and Improved Cell Sealing*. In: Solar Energy Materials & Solar Cells **94** (2010), p. 317-322.
 16. Tanaka, K., Oonuki, M., Moritake, N., Uchiki, H.: *Cu₂ZnSnS₄ Thin Film Solar Cells Prepared by Non-Vacuum Processing*. In: Solar Energy Materials & Solar Cells **93** (2009), p. 583-587.